Hue University Journal of Science: Natural Science
Vol. 132, No. 1D, 99–114, 2023

pISSN 1859-1388
eISSN 2615-9678

In silico extension on the antidiabetic potential of *Euonymus laxiflorus* natural compounds onto the inhibitability against protein tyrosine phosphatase 1B

Thanh Q. Bui[1], Nguyen Vinh Phu[2], Nguyen Thi Thanh Hai[1], Phan Tu Quy[3], Nguyen Thi Ai Nhung[1]*

[1] Department of Chemistry, University of Sciences, Hue University, Hue, Vietnam
[2] Faculty of Basic Sciences, University of Medicine and Pharmacy, Hue University, Hue, Vietnam
[3] Department of Natural Sciences & Technology, Tay Nguyen University, Buon Ma Thuot, Vietnam

* Correspondence to Nguyen Thi Ai Nhung <ntanhung@hueuni.edu.vn>
(*Received: 15 June 2023; Revised: 08 July 2023; Accepted: 19 July 2023*)

Abstract. *Euonymus laxiflorus* bioactive compounds 1-β-D-glucopyranosyloxy-3,5-dimethoxy-4-hydroxybenzene (**1**), Walterolactone A/B β-D-pyranoglucoside (**2**), Gallocatechin (**3**), Leonuriside A (**4**), Methyl galloate (**5**), and Catechin (**6**) were experimentally evidenced for their multi-inhibition against α-glucosidase and α-amylase. In this work, they were subjected to a combination of computational platforms on tyrosine phosphatase 1B (UniProtKB-PTP1B). As the results, the overall potentiality for bio-inhibitory applications is primarily evaluated by the order: **1** ($DS_{average}$ -12.2 kcal.mol^{-1}; polarisability 45.5 Å; no toxicity; ground-state energy -1222.73 a.u.; dipole moment 0.989 Debye) > **2** ($DS_{average}$ -9.7 kcal.mol^{-1}; polarisability 39.4 Å; no toxicity; ground-state energy -1070.08 a.u.; dipole moment 6.726 Debye) > **4** ($DS_{average}$ -9.1 kcal.mol^{-1}; polarisability 45.1 Å; no toxicity; ground-state energy -1222.73 a.u.; dipole moment 4.895 Debye). Altogether, the retrievals encourage further attempts to test the inhibitory effects of **2** against tyrosine phosphatase 1B and improve the dipole moment of **1** to enhance its biological applicability.

Keywords: antidiabetics, *Euonymus laxiflorus*, *in silico*, protein tyrosine phosphatase 1B

1 Introduction

Diabetes mellitus, a chronic glucose-related metabolic disorder, has risen as a worldwide health concern and is putting pressure on med-care systems worldwide. It not only creates hyperglycemia-related conditions but also induces further complications, which have been widely reported by preceding studies and clinical trials [1–5]. The mechanisms have also been well-established in the existing literature, including pancreatic β-cells deterioration (type 1) and insulin-metabolic abnormal activity (type 2); especially, the latter is responsible for 90-95 % of diagnoses [6]. Despite this well-rounded understanding, the cause is still highly uncertain; possible, genetic abnormalities, pathologic disorders, clinical conditions, or gestational failures are commonly referred and agreed by scientific community [7].

Up-to-date, there is no cure for this disease; the medicinal products on the market often only provide the temporary inhibition of undesirable biological activities, as symptomatic remedies rather than therapeutic treatments. The targets often relate to glucose- and insulin-based enzymes. For example, α-glucosidase is the bio-catalyst for the hydrolysis of -(1/4) and -(1/6) bonds in starch and disaccharide molecules; meanwhile, α-amylase is the major form of salivary and pancreatic amylase found in humans and other

mammals, responsible for the hydrolysis of α-linked polysaccharides (e.g. starch and glycogen) into shorter chains (e.g. dextrins and maltose). Their physiochemical roles induce the postprandial spikes from digestive carbohydrates [8,9]. From another view, protein tyrosine phosphatase 1B (PTP1B) catalyses the phosphorylation process, which further activates the glucose uptake of the insulin responsive cell [10]. Therefore, an effective bio-inhibitor against these proteins can provide negative regulatory effects on the hyperglycemic activity or insulin signaling pathway; consequently, a reduction of glucose uptake ensues. On the commercial market, there are various hypoglycemic drugs targeting α-glucosidase and α-amylase, e.g. Sulfonylureas, Biguanides, or Acarbose; however, the substances are also known either less effective towards the latter or with mild-serious side effects, e.g. diarrhea or flatulence [11,12]. Regarding the insulin-related enzyme, Trodusquemine, an aminosterol isolated from dogfish sharks, is the commonly known inhibitor with considerable efficacy [13]; however, the substance is only recently developed and also known for its expensive price. Therefore, looking for new and safe antidiabetic agents, especially those with multi-protein inhibitory effects, is still necessary. Natural sources, especially herbs and medicinal plants, are the subjects of research interest given their bioavailability and biodiversity.

Euonymus laxiflorus Champ. (the Celastraceae family) is a subtropical shrub (biome), native to South India, South China, Taiwan and the Indochinese peninsula. The plant is known by the local folk experiences for its medicinal value and has been long exploited in-practice as the remediation for osteoarthritis, inflammatory arthritis, and haemostasis. Nevertheless, only very recently, its anti-oxidant [14], anti-inflammatory [15], anti-cancerous [16], and anti-diabetic [17] activities have been proven scientifically by experimental evidences. In 2003, 11 components extracted and isolated from Taiwan-based *E. laxiflorus* aerial parts were first-time reported by Kou *et al.*. In 2017, the total methanol extract of *E. laxiflorus* Champ. trunk bark [14] and its major component (condensed tannin) [18] have observed with a hypoglycemic effect by Institute of Cancer Research (ICR) *in vivo* mouse model. In 2018, the antidiabetics against α-glucosidase and α-amylase [19] of 25 compounds identified in the methanol extracts of the bark of were evidenced by *in vitro* bioassays. Furthermore, the trials can be of more completeness if extended to all diabetes-related proteins in order to see whether the candidates also exhibit inhibitory effects against protein tyrosine phosphatase 1B. However, their high bio-versatility yet low content and the cost for PTP1B-based bioassays might put considerable challenges from the view of experimental trials.

With the aid of *in silico* science, the computer power can be wielded to significantly reduce the cost and time for equivalent wet lab-works. In bioinformatics, the promising candidates can be quickly allocated based on desirable properties. For example, molecular docking simulation is an efficient technique, with simple computational algorithms directly designed for prediction of ligand-protein interaction. It often neglects the influence of other bio-medium factors, e.g. dipole compatibility or polar sensibility. Fortunately, the latter was proved to be reconciled finely by incorporation of proper arguments on physicochemical properties [20,21]; meanwhile, the answer for the former is introduced in this report based on quantum chemical properties. Besides, quantum-based calculation can provide other useful molecular characteristics for argument on intermolecular and chemical tendencies of a studied molecule. Furthermore, there are statistically regressive models for predicting pharmacokinetics and pharmacological properties, which can serve as terminal descriptors to evaluate

pISSN 1859-1388
eISSN 2615-9678

drug-likeness and medicinal chemistry friendliness of candidate molecules. Altogether, these computational implementations if combined sufficiently and argued properly can provide a reliable view on the bio-compatible and pharma-suitable potentiality of a large number of compounds.

In this extension, candidates with multiple inhibitory effects against *α*-glucosidase and *α*-amylase experimentally reported by Nguyen *et al.* in 2018 [19] were selected for a computational screening for their potential towards protein tyrosine phosphatase 1B. In particular, the ligands were 1-β-D-glucopyranosyloxy-3,5-dimethoxy-4-hydroxybenzene (**1**), Walterolactone A/B β-D-pyranoglucoside (**2**), Gallocatechin (**3**), Leonuriside A (**4**), Methyl galloate (**5**), and Catechin (**6**); the targeted structure was UniProtKB-PTP1B; the platforms used were density functional theory (DFT) calculation, molecular docking simulation, and statistical regressions of physicochemical (using QSARIS) and pharmacological (using SwissADME) properties.

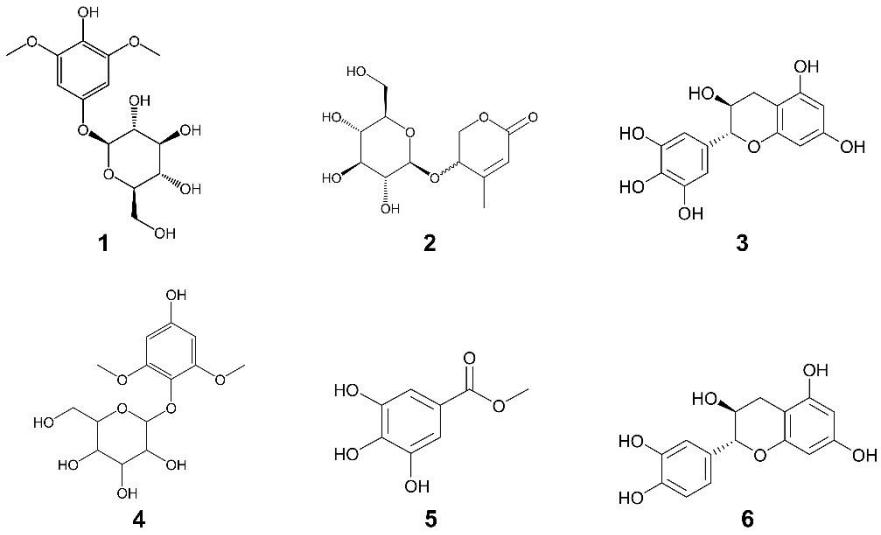

Fig. 1. Investigated compounds **1-6**

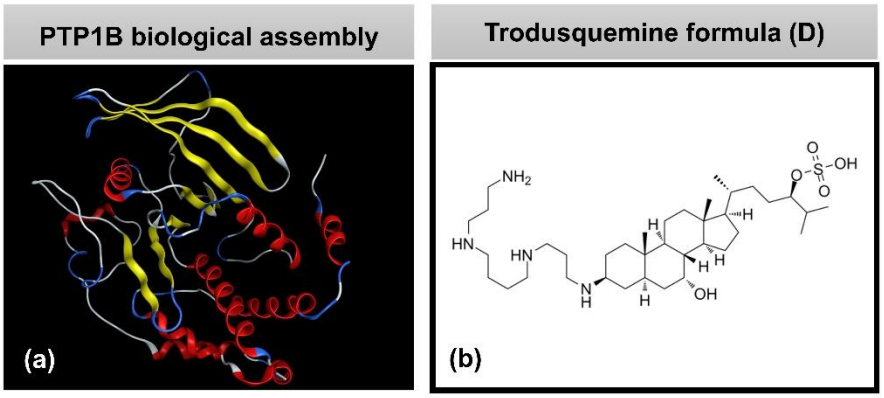

Fig. 2. (a) Biological assembly of PTP1B and (b) Trodusquemine (D)

2 Methodology

Biological assembly of protein tyrosine phosphatase 1B (PTP1B; ID: UniProtKB-A0A0U1XP67) and structural formula of Trodusquemin (**D**) are given in Figure 1; on the other side, chemical formulae of potential ligands (**1-6**) are presented in Figure 2. The data is from existing literature and altogether serve as the input for the computational screening in this study.

2.1 Molecular docking simulation

A typical procedure of molecular docking simulation (by MOE 2015.10 [22]) follows three steps, i.e.: (i) Input preparation (configuration: protein active range 4.5 Å, ligand charge-assigning using Gasteiger-Huckel method); (ii) Docking simulation (configuration: retaining poses 10; solutions per iteration 1000; solutions per fragmentation 200); (iii) Re-docking iteration (threshold: root-mean-square deviation (RMSD) values < 2 Å). Given theoretical interpretation, the inhibitory effectiveness of a ligand towards the targeted protein structure can be primarily evaluated by docking score (DS) energy of the associated inhibitory system, which represents pseudo-Gibbs free energy (formed by hydrophilic binding and hydrophobic interaction); also, RMSD values and number of hydrogen-like interactions can be considered for arguments on bio-conformational rigidity and binding strength, respectively. In addition, MOE can provide visual rendering for ligand-protein interaction maps (2D) and in-pose arrangements (3D).

2.2 QSARIS-based analysis

Drug-likeness properties of the phytochemicals were predicted by a combinational model, including (i) Parameters: QSARIS-derived physical properties (based on Gasteiger–Marsili method [23]); (ii) Reference: Lipinski's rule of five [24]. The former includes molecular mass (Da), polarizability (Å^3), size (Å), and dispersion coefficients (log*P* and log*S*). The latter provides the theoretical criteria for a well membrane-permeable candidate, i.e.: molecular mass < 500 Da; hydrogen-bond donors ≤ 5; hydrogen-bond acceptors ≤ 10; log*P* < +5 [25,26].

2.3 ADMET analysis

Pharmacological potentiality of the compounds was also assessed by a combinational model, including (i) ADMET properties: absorption, distribution, metabolism, excretion, and toxicity; (ii) Reference: Pires' theoretical interpretations [27]. The parameters were obtained from a web-based regressive model, developed and maintained by Molecular Modeling Group, Swiss Institute of Bioinformatics, i.e. SwissADME (http://www.swissadme.ch/; 9th June 2023). The document provides thresholds for the pharmacokinetic behaviour of each candidate.

2.4 Density functional theory calculation

Molecular chemical properties of the investigated structures were given by density functional theory (DFT) calculation using Gaussian 09 without symmetry constraints [28]. Level of theory M052X/6–311++G(d,p) and basis set def2-TZVPP [29] were selected. The converged geometries were checked for the structural global minimum on the potential energy surface (PES) by vibrational frequencies. The frozen-core approximation for non-valence-shell electrons was applied. The resolution-of-identity (RI) approximation was set. The frontier orbital analysis was carried out by NBO 5.1 at the level of theory M052X/def2-TZVPP.[30].

pISSN 1859-1388
eISSN 2615-9678

3 Results and discussion

3.1 Docking-based inhibitability

The most susceptible sites of the targeted protein are highlighted in Figure 3. The results from docking simulation can be utilized for argument on the inhibitory effects of each compound (**1-6**) against the protein structure for tyrosine-protein phosphatase type 1 (PTP1B). In this scope, the total docking score (DS) values and the number of hydrogen-like bonds are selected as the main indicators for inhibitory effectiveness, which respectively represent pseudo values for Gibbs free energy of ligand-protein complex formation and their strong intermolecular bonds.

The primary docking parameters are summarised in Table 1; the control drug (**D**) is Trodusquemine. Overall, different compounds exhibit different affinities toward the sites of PTP1B, especially Site 1 (majority of candidates) and Site 4 (1 and D). The average values are considered as the representative for in-practice inhibitory effectiveness since the biological process is often based on multi-site inhibition rather than single-site selectiveness. In principle, sufficient distortion forces channelling on a variety of protein sites would result in denaturation of enzyme shape, thus enzymatic cease ensuing in overall. Given this argument, the most effective inhibitors against PTP1B are predicted by the order: **1-PTP1B** ($DS_{average}$ -12.2 kcal.mol^{-1}) > **3-PTP1B** ($DS_{average}$ -10.4 kcal.mol^{-1}) > **2-PTP1B ≈ 5-PTP1B** ($DS_{average}$ ca. -9.5 kcal.mol^{-1}) > **4-PTP1B ≈ 6-PTP1B** ($DS_{average}$ ca. -9.1 kcal.mol^{-1}). These figures are significantly elevated cf. that of **D-PTP1B** ($DS_{average}$ -8.7 kcal.mol^{-1}). Generally speaking, this indicates that all the candidates are highly promising as pervasive bio-inhibitors against the structure.

Table 1. Results on inhibitability of **1-6** and **D** toward PTP1B sites

Complex	Site 1		Site 2		Site 3		Site 4		Average
	E	N	E	N	E	N	E	N	E
1-PTP1B	-11.9	4	-11.0	3	-12.0	4	**-13.9**	**8**	-12.2
2-PTP1B	**-12.0**	**5**	-8.3	2	-9.4	3	-8.9	2	-9.7
3-PTP1B	-10.7	3	-9.4	2	**-12.2**	**5**	-9.3	2	-10.4
4-PTP1B	**-11.2**	**4**	-9.0	2	-8.4	2	-7.6	1	-9.1
5-PTP1B	**-11.4**	**4**	-9.5	2	-9.3	2	-8.0	1	-9.6
6-PTP1B	-8.8	2	-8.6	2	-8.0	1	**-11.3**	**4**	-9.2
D-PTP1B	-6.4	0	-7.5	0	-9.8	2	**-10.9**	**3**	-8.7

E: DS value (kcal.mol^{-1}); **N**: Number of hydrophilic interactions

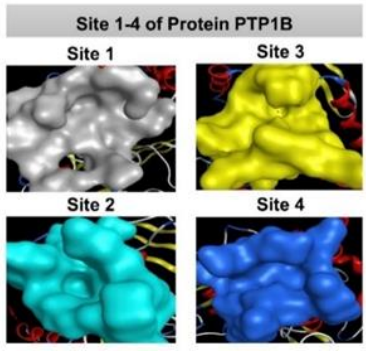

Fig. 3. Quaternary structures of PTP1B with the approachable sites by the ligands: Site 1 (gray), Site 2 (cyan), Site 3 (yellow), Site 4 (blue)

The most stable complexes regarding each ligand-protein system are selected for more in-detail presentation, whose data is given in Table 2. These should be considered as the main inhibitory products in practice given their lowest pseudo formation energy (aka. DS value). Following this consideration, the order (ligand-protein.site) for inhibitory potential is: **1-PTP1B.4** (DS -13.9 kcal.mol^{-1}; hydrophilic bonds 8) > **2-PTP1B.1** ≈ **3-PTP1B.3** (DS ca. -12 kcal.mol^{-1}; hydrophilic bonds 5) > **4-PTP1B.1** ≈ **5-PTP1B.1** ≈ **6-PTP1B.4** (DS ca. -11 kcal.mol^{-1}; hydrophilic bonds 4). Particularly, although **1** exhibits the similar affinity tendency with **D** (towards Site 4), its effectiveness (represented by DS value and number of hydrogen-like bonds) is predominant. From another perspective, the RMSD of backbone lengths (after re-docking iterations) might further imply the capacity of the ligands to alter the targeted protein structure, which can be ranked into the order: **4** (RMSD 1.57 Å) > **1** (RMSD 1.22 Å) > **3** ≈ **5** ≈ **6** (RMSD ca. 1.15 Å) > **2** (RMSD 0.81 Å). Besides, the amino acid residues associated with noticeably low individual formation free energy (e.g. **1-PTP1B.4**: Glu 252, -3.2 kcal.mol^{-1}; **2-PTP1B.1**: Asp 29, -3.6 kcal.mol^{-1}; **5-PTP1B.1**: Lys 36, -5.3 kcal.mol^{-1}; **6-PTP1B.4**: Lys 248, -4.8 kcal.mol^{-1}) can be considered as potential secondary targets if the compounds are selected for drug design phase.

The ligand-protein configurations are also visually rendered, presented in Figure 4. The descriptive specification includes hydrogen-like bonding (dashed arrow), van de Waals interaction (blurry purple), and conformational fitness (dashed contour). The 3D in-site arrangements show that the sites are rather open and spacious, compared to the inhibitor sizes. This implicates that further modification/functionalization on the current ligand structures is still possible. From 2D maps, the ligands are likely to have good conformational fitness with the in-site features given by the continuousness of dashed contours.

Table 2. Docking results for most effective ligands-PTP1B inhibitory complexes

Ligand-protein complex			**Hydrogen bond**					**van der Waals interaction**
Complex	**DS**	**RMSD**	**L**	**P**	**T**	**D**	**E**	
1- PTP1B	-13.9	1.22	O	O Ser243	H-donor	3.16	-1.6	Glu75, Leu234, Val249, Asp245, Lys255
			O	O Glu76	H-donor	2.95	-2.4	
			O	O Glu76	H-donor	2.81	-0.8	
			C	O Glu76	H-donor	3.23	-1.0	
			O	O Glu252	H-donor	2.89	-3.2	
			O	N Arg238	H-acceptor	2.98	-1.6	
			O	N Arg238	H-acceptor	2.71	-3.1	
			O	C Lys248	H-acceptor	3.11	-1.1	
2-PTP1B	-12.0	0.81	O	O Asp29	H-donor	2.84	-2.5	Tyr20, Ile261, Gly259, Met258, Asp48, Phe52, Ser28, Ala27
			O	O Asp29	H-donor	2.90	-3.6	
			O	N Arg24	H-acceptor	3.00	-2.3	
			O	N Arg254	H-acceptor	3.36	-1.4	
			O	N Gln262	H-acceptor	2.86	-0.9	

pISSN 1859-1388
eISSN 2615-9678

Ligand-protein complex			Hydrogen bond						van der Waals interaction
Complex	**DS**	**RMSD**	**L**	**P**		**T**	**D**	**E**	
3-PTP1B	-12.2	1.17	O	O	Ser80	H-donor	3.09	-0.6	His208, Gly209, Ser205, Pro206, Leu204, Arg79, Lys73, Leu71, Lys103, Glu101
			O	O	Gln102	H-donor	3.04	-1.5	
			O	O	Gln78	H-donor	2.92	-0.9	
			6-ring	C	Ser80	π -H	3.88	-0.9	
			6-ring	C	Pro210	π -H	3.16	-0.9	
4- PTP1B	-11.2	1.57	O	O	Asp48	H-donor	3.05	-0.7	Ser28, Phe52, Arg254, Tyr20, Ile219, Val49, Gly259, Met258, Gln262
			O	O	Asp48	H-donor	2.94	-3.1	
			O	O	Asp29	H-donor	3.33	-1.0	
			O	N	Arg24	H-acceptor	2.95	-0.9	
5- PTP1B	-11.4	1.14	O	N	Lys36	H-acceptor	2.94	-5.3	Asp29, Pro31, Phe30, Met258, Arg47, Val49, Ser50
			O	C	Asp48	H-acceptor	3.39	-0.7	
			O	N	Cys32	H-acceptor	3.19	-0.8	
			O	N	Lys36	ionic	2.94	-4.9	
6-PTP1B	-11.3	1.15	O	O	Glu75	H-donor	3.09	-0.8	Glu252, Val249, Val244, Arg238, Glu76
			O	O	Ser243	H-donor	2.95	-1.5	
			O	N	Asp245	H-acceptor	3.20	-0.9	
			O	N	Lys248	H-acceptor	3.01	-4.8	
D- PTP1B	-10.9	1.14	O	O	Glu75	H-donor	3.36	-3.5	Asp245, Arg238, Val244, Ser243, Val249, Leu234, Leu251, Glu252, Phe256, Glu76, Glu26, Ser28, Phe30
			N	C	Lys298	H-acceptor	3.22	-1.8	
			O	N	Lys255	H-acceptor	3.10	-1.2	

DS: Docking score energy (kcal.mol^{-1}); **RMSD**: Root-mean-square deviation (Å);
L: Ligand; **P**: Protein; **T**: Type; **D**: Distance (Å); **E**: Energy (kcal.mol^{-1})

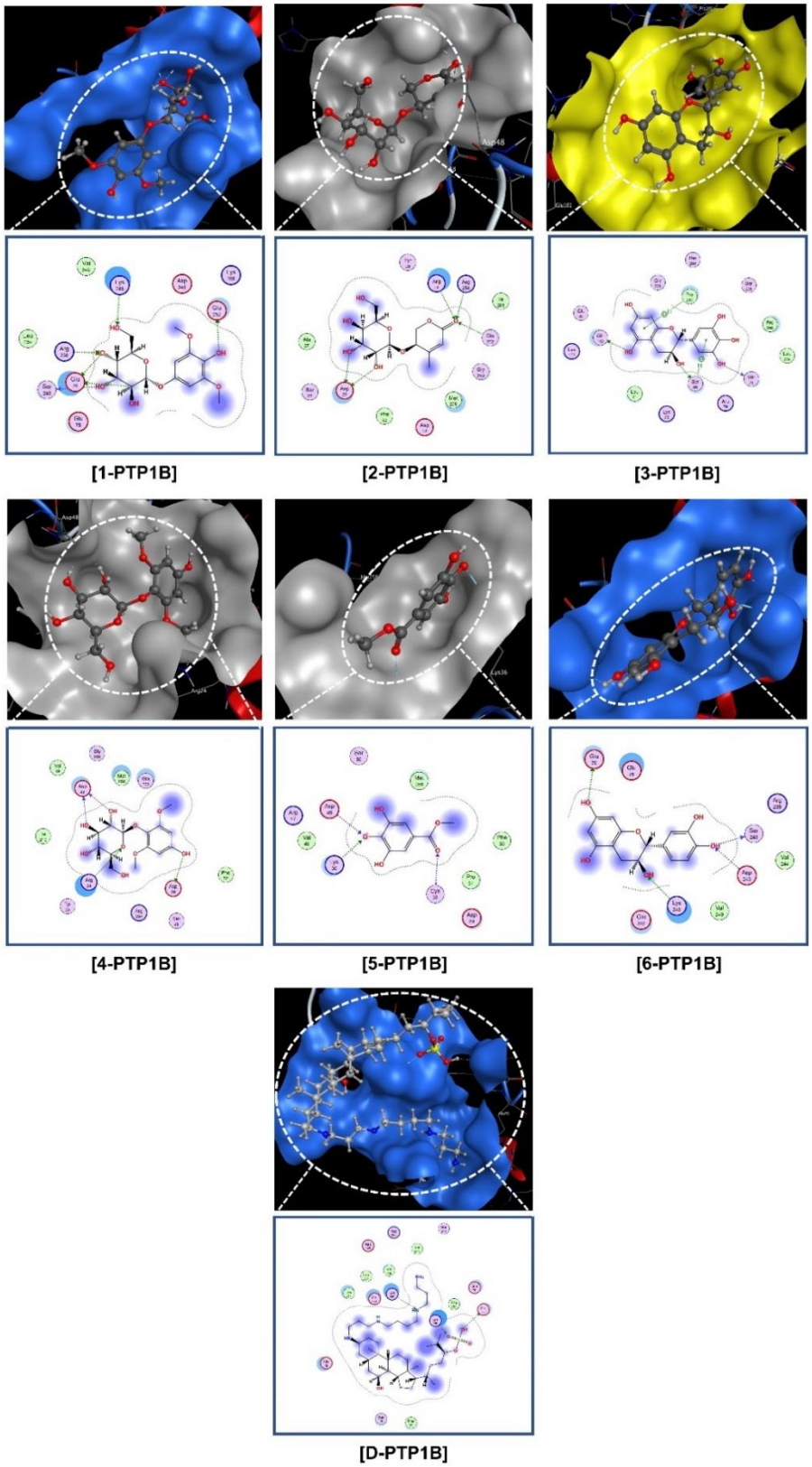

Fig. 4. Visual presentation and in-pose interaction map of ligand-PTP1B (ligand: **1-6** and **D**) inhibitory structures

pISSN 1859-1388
eISSN 2615-9678

3.2 QSARIS-based physicochemical properties

The physicochemical properties of the compounds (retrieved from the QSARIS) and the number of hydrogen bonds (counted from docking-based results) are given in Table 3. Overall, all the candidates well satisfy Lipinski's criteria for the argument on drug-likeness, i.e.: molecular mass < 500 amu; hydrogen-like donors < 5; hydrogen-like acceptors < 10; partition coefficient log$P$ < +5. From the view of biological compatibility, **1**, **2**, **4** are considered as most promising given by their lowest octane-water partition ratios (log$P$ < 0). From the view of biological interactability, the potential can be ranked by the order of polarisability: **1** ≈ **4** (ca. 45 Å) > **2** ≈ **3** ≈ **6** (ca. 40 Å) > **5** (22.8 Å). The property represents the sensitivity of a structure to external electric fields such as those created by other polarised agents (e.g. amino-acid-based protein structures); the unit conversion is given by Claussius-Mossotti relation: $10^6/4\pi\epsilon_0$ $[\mathrm{A}^2.\mathrm{s}^4.\mathrm{kg}^{-1}] \equiv 1\ [\mathrm{cm}^3]$ [31].

Table 3. Physicochemical properties of **1-6**

Compound	Mass (amu)	Polarisability (Å^3)	Size (Å)	Dispersion coefficients		Total interaction* (PTP1B)		
				Log$P$	Log$S$	H-donor	H-acceptor	H-π
1	332.3	45.5	372.1	-0.99	-0.54	3	5	0
2	290.1	39.4	356.2	-2.09	-0.18	3	2	0
3	306.3	41.4	368.5	1.71	-1.37	0	3	2
4	332.3	45.1	370.6	-1.49	-0.54	1	3	0
5	184.3	22.8	203.1	1.11	-0.94	3	0	0
6	290.2	40.5	312.5	1.98	-1.74	2	2	0

*counted from docking results of each most effective ligand-PTP1B inhibitory complex

Table 4. Pharmacokinetic and pharmacological properties of **1-6**

Property	1	2	3	4	5	6	Unit
Absorption							
Water solubility	-2.267	-1.031	-3.09	-2.203	-2.001	-3.179	(1)
Caco2 permeability	-0.093	-0.187	-0.521	-0.195	-0.056	-0.292	(2)
Intestinal absorption	32.191	40.937	65.102	34.57	76.635	73.244	(3)
Skin Permeability	-2.735	-3.082	-2.735	-2.741	-2.771	-2.736	(4)
P-glycoprotein substrate	Yes	No	Yes	Yes	Yes	Yes	(5)
P-glycoprotein I inhibitor	No	No	No	No	No	No	(5)
P-glycoprotein II inhibitor	No	No	No	No	No	No	(5)

Property	1	2	3	4	5	6	Unit
Distribution							
VDss	0.095	-0.161	0.229	-0.047	0.355	0.675	(6)
Fraction unbound	0.498	0.748	0.167	0.509	0.615	0.156	(6)
BBB permeability	-1.228	-0.96	-1.512	-1.375	-1.046	-1.017	(7)
CNS permeability	-4.7	-4.415	-3.703	-4.673	-3.376	-3.314	(8)
Metabolism							
CYP2D6 substrate	No	No	No	No	No	No	(5)
CYP3A4 substrate	No	No	No	No	No	No	(5)
CYP1A2 inhibitor	No	No	No	No	No	No	(5)
CYP2C19 inhibitor	No	No	No	No	No	No	(5)
CYP2C9 inhibitor	No	No	No	No	No	No	(5)
CYP2D6 inhibitor	No	No	No	No	No	No	(5)
CYP3A4 inhibitor	No	No	No	No	No	No	(5)
Excretion							
Total Clearance	0.735	1.456	0.454	0.72	0.635	0.254	(9)
Renal OCT2 substrate	No	No	No	No	No	No	(5)
Toxicity							
AMES toxicity	No	No	Yes	No	Yes	Yes	(5)
Max. tolerated dose	0.5	0.924	0.749	0.402	-0.296	0.542	(10)
hERG I inhibitor	No	No	No	No	No	No	(5)
hERG II inhibitor	No	No	No	No	No	No	(5)
Oral Rat Acute Toxicity	2.725	2.014	2.17	2.787	1.898	2.103	(11)
Oral Rat Chronic Toxicity	3.89	3.42	2.988	4.367	2.432	2.759	(12)
Hepatotoxicity	No	No	No	No	No	No	(5)
Skin Sensitisation	No	No	No	No	No	No	(5)
T. Pyriformis toxicity	0.285	0.285	0.307	0.285	0.195	0.335	(13)
Minnow toxicity	4.682	3.622	1.543	3.719	2.871	1.947	(14)

(1) log mol.L^{-1}; (2) log Papp (10^{-6} cm.s^{-1}); (3) %; (4) log Kp; (5) Yes/No; (6) log L.kg^{-1}; (7) log BB; (8) log PS;
(9) log mL.min^{-1}.kg^{-1}; (10) log mg.kg^{-1}.day^{-1}; (11) mol.kg^{-1}; (12) log mg.kg^{-1}_bw.day^{-1}; (13) log μg.L^{-1}; (14) log mM

3.3 ADMET-based pharmacokinetics and pharmacology

The ADMET properties of the compounds are summarised in Table 4, categorised into absorption, distribution, metabolism, excretion, and toxicity. The thresholds for theoretical prediction are based on Pires' interpretations [27]. All the candidates are considered suitable for oral

pISSN 1859-1388
eISSN 2615-9678

intake given by their high absorbability (intestinal absorption > 30 %) and low resistance (Caco2 permeability < 8×10^{-8} cm. s^{-1}); none of them is predicted to inhibit the activity of P-glycoprotein family, thus no effect on the extrusion of the toxins and xenobiotics out of cells. The compounds do not show noticeable tendency of accumulation to either tissue or plasma (by relatively balanced VDss); in addition, they are unlikely to cross the blood-brain barrier (logBB < -1) or penetrate the central nervous system (logPS < -3). None of them is predicted to either inhibit the activity of the cytochromes P450 family or be oxidised by the liver (as their substrates); also, they are unlikely to be rapidly excreted by the kidney (carried by organic cation transporter 2). These bio-kinetic behaviour might be conducive to their prolong circulation in the body, thus longer medicinal effects. However, toxicity-based predictions pose certain precautions for pharmacological development. While **1**, **2**, and **4** are particularly safe for medicinal use, i.e.: (i) no mutagenic potentials; (ii) no potential for fatal ventricular arrhythmia as hERG inhibitors; (ii) no hepatotoxicity; (iv) no skin sensitisation; (v) toxicity to bacterium *T. Pyriformis* (pIGC50 > -0.5 log μg.L^{-1}) yet safety to animal organisms, e.g. fish Flathead Minnows (LC50 > -0.3), the model expects **3**, **5**, and **6** might act as carcinogens. This means that if the latter three were selected for further consideration, they should be subjected to more in-depth assessments of mutagenicity.

3.4 Quantum-based chemical properties

The results from quantum calculation provide another view on the bio-medium compatibility and intermolecular interactability of the candidates based on *ab initio* insights of their chemical properties.

The optimised geometries of the bioactive compounds are shown in Figure 5. Overall, the input structures can be self-consistently converged easily without any geometrical constraints or abnormal bonding parameters (i.e. angles and length). This is often of the characteristics of natural compounds; thereby in-turn also validating their spectroscopic characterisation and structural elucidation from the preceding works.

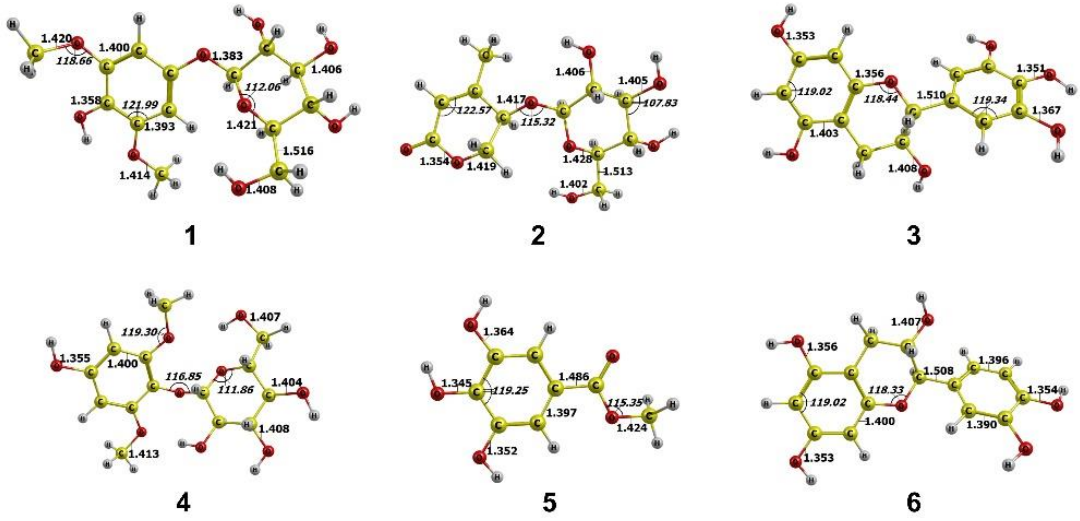

Fig. 5. Geometrically optimised structure of **1-6**; Units: bond length (Å), bond angle (°)

Table 5. Ground state electronic energy and dipole moment values of **1-6**

Compound	**Ground state electronic energy** (a.u.)	**Dipole moment** (Debye)
1	-1222.729	0.898
2	-1070.083	6.726
3	-1106.794	4.231
4	-1222.728	4.895
5	-685.919	1.714
6	-1031.551	2.602

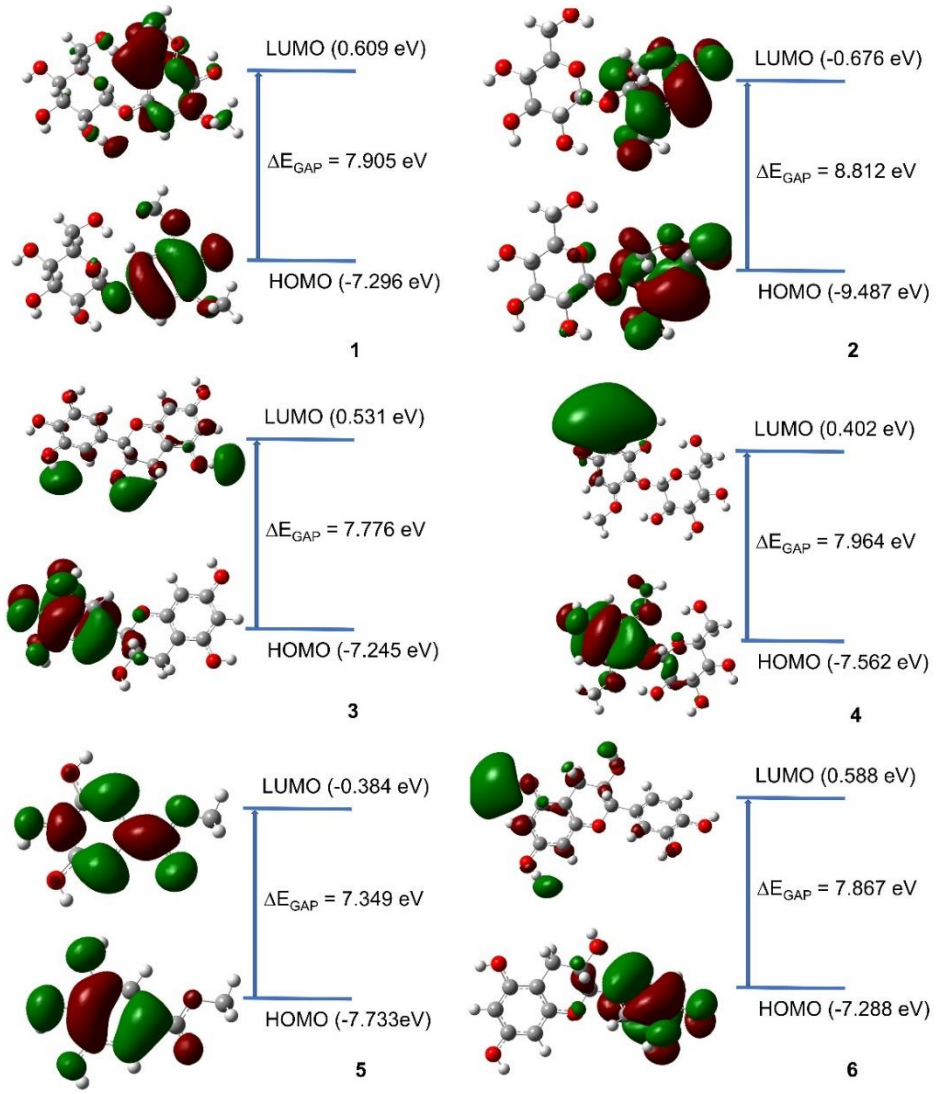

Fig. 6. Frontier molecular orbitals (HOMO and LUMO) of **1-6**

pISSN 1859-1388
eISSN 2615-9678

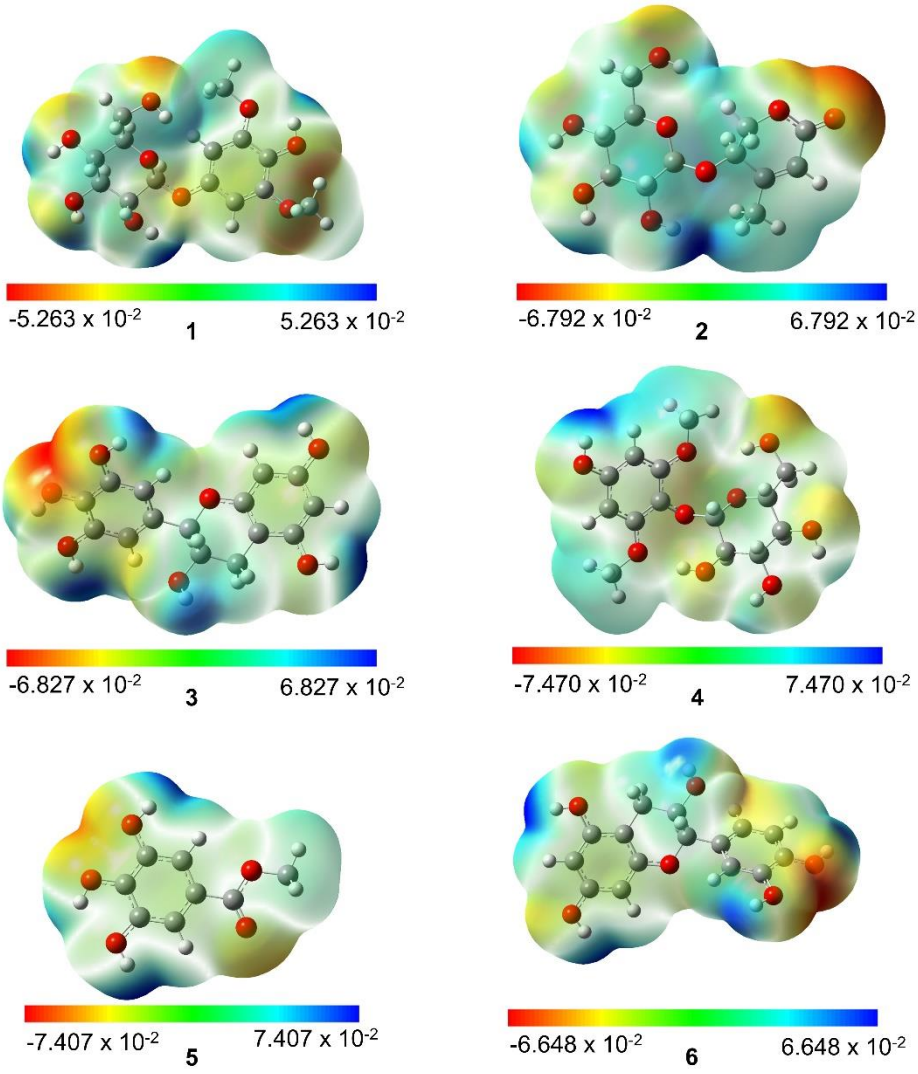

Fig. 7. Molecular electrostatic potential (MEP) maps of 1-6

The molecular properties are summarised in Table 5, including ground state energy and dipole moment. In essence, the former represents the overall chemical activeness and the latter is the positive-negative charge separation in a system, thus measuring the compatibility with dipole-solvent environments (e.g. physio-chemical media). From this standpoint, **5** is the most active chemically given its highest ground-state energy (-685.92 a.u.). This equals to the interpretation that it holds the lowest potential for bio-inhibitory applications since the molecule possibly reacts with the body chemicals before reaching the targeted protein. In contrast, **1** and **4** (ca. -1222 a.u.) most likely retain their structural elements in biological media to serve as bio-inhibitors. The dipole-environment compatibility of **1** is the lowest, given by its dipole moment value (0.898 Debye); on the other hand, the highest value (6.726 Debye) of **2** can be translated into the most promising. Nevertheless, the exceptional inhibitability (predicted by docking-based technique) of **1** still considerably outweighs its weakness (argued by quantum-based calculation), thereby justifying the efforts to enhance its compatibility via molecular functionalisation.

The highest occupied molecular orbital (HOMO) and lowest unoccupied molecular orbital

(LUMO) of the studied structures are shown in Figure 6, with their band-gap energy (ΔE_{GAP}). The value can be considered as an indicator for the intermolecular binding capability towards protein structures since the polypeptide molecules were known and proved with electric conductivity, explained by the electron tunneling mechanism [32,33]. In other words, lower figures indicate higher ligand-protein electric fusion, thus stronger electric binding. Overall, the values lie on the transition of an insulator (> 9 eV) and a semiconductor (< 3.2 eV) [34] following the effective order: **5** (7.349 eV) > **3** ≈ **6** (ca. 7.8 eV) > **1** ≈ **4** (ca. 7.9 eV) > **2** (8.812 eV).

Molecular electronic potential (MEP) maps of the structures are given in Figure 7, providing the distribution of chemical activities over each molecular plane. By convention, reddish colours represent the negative electrostatic potential (i.e. rich in electron density); this means that the regions might serve as a nucleophilic site in chemical reactions yet an electron donor in intermolecular interactions. In contrast, bluish colours represent positive electrostatic potential (i.e. related to electrophilic reactivity). Otherwise, whitish colours represent the neutral regions (unlikely to position either of the tendencies). It can be seen that **1**, **2**, and **3** can swap the chemical tendencies rather arbitrarily and consecutively over their molecular planes. From a theoretical standpoint, this characteristic might, to a certain degree, measure their flexibility when in physical interactions with external complex structures, such as protein-based folded conformations.

4 Conclusions

This study extends the diabetic potentiality of *Euonymus laxiflorus* bioactive compounds (**1-6**), which were already experimentally evidenced with as promising α-glucosidase and α-amylase inhibitors, onto tyrosine phosphatase 1B (UniProtKB-PTP1B). Molecular docking simulation predicts the most effective ligand-PTP1B inhibitory systems: **1-PTP1B** ($DS_{average}$ -12.2 kcal.mol^{-1}) > **3-PTP1B** ($DS_{average}$ -10.4 kcal.mol^{-1}) > **2-PTP1B** ($DS_{average}$ -9.7 kcal.mol^{-1}). Physicochemical analysis justifies the drug-likeness of all candidates; particularly, polarisability reasons for their bio-inhibitory applicability: **1** ≈ **4** (ca. 45 Å) > **2** ≈ **3** ≈ **6** (ca. 40 Å). ADMET pharmacokinetics discourages the use of **3**, **5**, and **6** due to their mutagenic potentials. Quantum-based chemical properties especially encourage the bio-medium applications of **2** (ground state -1070.08 a.u.; dipole moment 6.726 Debye) and **4** (ground state -1222.73 a.u.; dipole moment 4.895 Debye) by their chemical stability and dipole-environment compatibility. Altogether, the theoretical screening specifies 1-β-D-glucopyranosyloxy-3,5-dimethoxy-4-hydroxybenzene (**1**) and Walterolactone A/B β-D-pyranoglucoside (**2**) as the promising versatile agents for anti-diabetic applications, serving as multi-purpose inhibitors acting effectively on different diabetes-related protein structures (i.e. α-glucosidase, α-amylase, and tyrosine phosphatase 1B).

Acknowledgement

This work was funded by Hue University [Grant number DHH2022-01-198]. Nguyen Thi Ai Nhung acknowledges the support of Hue University under the Core Research Program [Grant number NCM.DHH.2020.04].

Conflicts of interest

The authors declare that there is no conflict of interest regarding the publication of this article.

References

1. Abraira C, Colwell JA, Nuttall FQ, Sawin CT, Nagel NJ, Comstock JP, et al. Veterans Affairs Cooperative

pISSN 1859-1388
eISSN 2615-9678

Study on glycemic control and complications in type II diabetes (VA CSDM): results of the feasibility trial. Diabetes Care. Am Diabetes Assoc. 1995;18:1113-23.

2. Ohkubo Y, Kishikawa H, Araki E, Miyata T, Isami S, Motoyoshi S, et al. Intensive insulin therapy prevents the progression of diabetic microvascular complications in Japanese patients with non-insulin-dependent diabetes mellitus: a randomized prospective 6-year study. Diabetes Res Clin Pract. Elsevier. 1995;28:103-17.
3. Klein R, Klein BEK, Moss SE, Cruickshanks KJ. Relationship of hyperglycemia to the long-term incidence and progression of diabetic retinopathy. Arch Intern Med. American Medical Association. 1994;154:2169-78.
4. Wu Y, Ding Y, Tanaka Y, Zhang W. Risk Factors Contributing to Type 2 Diabetes and Recent Advances in the Treatment and Prevention. International Journal of Medical Sciences. 2014;11(11):1185-200.
5. Sandholm N, Forsblom C. Genetics of Diabetic Microvascular Disease. Microvascular Disease in Diabetes; 2020. p. 23-44.
6. Henning RJ. Type-2 diabetes mellitus and cardiovascular disease. Future Cardiol. Future Medicine; 2018;14:491-509.
7. Draznin B, Aroda VR, Bakris G, Benson G, Brown FM, Freeman R, et al. 2. Classification and Diagnosis of Diabetes: Standards of Medical Care in Diabetes-2022. Diabetes Care. 2022;45:S17-38.
8. Holman RR, Cull CA, Turner RC. A randomized double-blind trial of acarbose in type 2 diabetes shows improved glycemic control over 3 years (U.K. Prospective Diabetes Study 44). Diabetes Care. 1999;22(6):960-4.
9. Lebovitz HE. Alpha-glucosidase inhibitors. Endocrinology and Metabolism Clinics of North America. 1997;26(3):539-51.
10. Vieira MNN, Lyra e Silva NM, Ferreira ST, De Felice FG. Protein tyrosine phosphatase 1B (PTP1B): a potential target for Alzheimer's therapy?. Front Aging Neurosci. 2017;9.
11. Özil M, Emirik M, Etlik SY, Ülker S, Kahveci B. A simple and efficient synthesis of novel inhibitors of alpha-glucosidase based on benzimidazole skeleton and molecular docking studies. Bioorganic Chemistry. 2016;68:226-35.
12. Nikookar H, Mohammadi-Khanaposhtani M, Imanparast S, Faramarzi MA, Ranjbar PR, Mahdavi M, et al. Design, synthesis and in vitro α-glucosidase inhibition of novel dihydropyrano [3, 2-c] quinoline derivatives as potential anti-diabetic agents. Bioorganic Chemistry. 2018;77:280-6.
13. Cho H. Protein tyrosine phosphatase 1B (PTP1B) and obesity. Vitam Horm. 2013;91:405-24.
14. Nguyen Q-V, Nguyen N-H, Wang S-L, Nguyen VB, Nguyen AD. Free radical scavenging and antidiabetic activities of Euonymus laxiflorus Champ. extract. Res Chem Intermed. 2017;43:5615-24.
15. Nguyen VB, Wang S-L, Nguyen AD, Lin Z-H, Doan CT, Tran TN, et al. Bioactivity-guided purification of novel herbal antioxidant and anti-NO compounds from Euonymus laxiflorus Champ. Molecules. 2018;24:120.
16. Kuo Y-H, Huang H-C, Chiou W-F, Shi L-S, Wu T-S, Wu Y-C. A Novel NO-Production-Inhibiting Triterpene and Cytotoxicity of Known Alkaloids from Euonymus l axiflorus. J Nat Prod. 2003;66:554-7.
17. Nguyen VB, Nguyen QV, Nguyen AD, Wang S-L. Screening and evaluation of α-glucosidase inhibitors from indigenous medicinal plants in Dak Lak Province, Vietnam. Res Chem Intermed. 2017;43:3599-612.
18. Nguyen VB, Wang S-L, Nguyen TH, Nguyen MT, Doan CT, Tran TN, et al. Novel potent hypoglycemic compounds from Euonymus laxiflorus Champ. and their effect on reducing plasma glucose in an ICR mouse model. Molecules. 2018;23:1928.
19. Nguyen VB, Wang S-L, Nguyen AD, Vo TPK, Zhang L-J, Nguyen QV, et al. Isolation and identification of novel α-amylase inhibitors from Euonymus laxiflorus Champ. Res Chem Intermed. 2018;44:1411-24.
20. Thao TTP, Bui TQ, Quy PT, Bao NC, Van Loc T, Van Chien T, et al. Isolation, semi-synthesis, docking-based prediction, and bioassay-based activity of Dolichandrone spathacea iridoids: new catalpol derivatives as glucosidase inhibitors. RSC Adv. 2021;11:11959-75.
21. Thao TTP, Bui TQ, Hai NTT, Huynh LK, Quy PT, Bao NC, et al. Newly synthesised oxime and lactone derivatives from Dipterocarpus alatus dipterocarpol as anti-diabetic inhibitors: experimental bioassay-based evidence and theoretical computation-based prediction. RSC Adv. 2021;11:35765-82.

22. Molecular Operating Environment (MOE), 2015.02 Chemical Computing Group ULC. Montreal: Chemical Computing Group ULC; 2015.

23. 2Gasteiger J, Marsili M. Iterative partial equalization of orbital electronegativity-a rapid access to atomic charges. Tetrahedron. 1980;36:3219-28.

24. Lipinski CA, Lombardo F, Dominy BW, Feeney PJ. Experimental and computational approaches to estimate solubility and permeability in drug discovery and development settings. Adv Drug Deliv Rev. 1997;23:3-25.

25. Ahsan MJ, Samy JG, Khalilullah H, Nomani MS, Saraswat P, Gaur R, et al. Molecular properties prediction and synthesis of novel 1,3,4-oxadiazole analogues as potent antimicrobial and antitubercular agents. Bioorganic Med Chem Lett. 2011;21:7246-50.

26. Mazumdera J, Chakraborty R, Sena S, Vadrab S, Dec B, Ravi TK. Synthesis and biological evaluation of some novel quinoxalinyl triazole derivatives. Der Pharma Chem. 2009;1:188-98.

27. Pires DEV, Blundell TL, Ascher DB. pkCSM: Predicting small-molecule pharmacokinetic and toxicity properties using graph-based signatures. J Med Chem. 2015;58:4066-72.

28. Gaussian 09, Revision A.02. Wallingford: Gaussian Inc; 2016

29. Markovi ZS, Dimitri JM. Mechanistic study of the structure – activity relationship for the free radical scavenging activity of baicalein. J Mol Model. 2011;17:2575-84.

30. Weigend F, Ahlrichs R. Balanced basis sets of split valence, triple zeta valence and quadruple zeta valence quality for H to Rn: Design and assessment of accuracy. Phys Chem Chem Phys. 2005;7:3297-305.

31. Reed AE, Weinstock RB, Weinhold F. Natural population analysis. J Chem Phys. 1985;83:735-46.

32. Feynman R. The Feynman lectures on physics - Volume II. Millenium. Gottlieb MA, editor. New York: Basic Books; 2010.

33. Rosenberg B. Electrical Conductivity of Proteins. Nature. 1962;193:364-5.

34. 3Kharkyanen VN, Petrov EG, Ukrainskii II. Donor-Acceptor model of electron transfer through proteins. J Theor Biol. 1978;73:29-50.

35. Suresh BV. Solid State Devices and Technology. Bangalore: Pearson Education India; 2010.